THE JOURNAL OF BIOLOGICAL CHEMISTRY
Vol. 279, No. 6, Issue of February 6, pp. 4903–4912, 2004
Printed in U.S.A.

Crystal Structure of Octaprenyl Pyrophosphate Synthase from Hyperthermophilic *Thermotoga maritima* and Mechanism of Product Chain Length Determination*

Received for publication, September 12, 2003, and in revised form, November 7, 2003
Published, JBC Papers in Press, November 15, 2003, DOI 10.1074/jbc.M310161200

Rey-Ting Guo‡§, Chih-Jung Kuo¶, Chia-Cheng Chou¶‖, Tzu-Ping Ko¶, Hui-Lin Shr¶‖, Po-Huang Liang‡§¶, and Andrew H.-J. Wang‡§¶‖‡‡**

From the ‡Taiwan International Graduate Program, Academia Sinica, Taipei 115, Taiwan, §Institute of Biochemical Sciences, National Taiwan University, Taipei 106, Taiwan, and ¶Institute of Biological Chemistry and ‖Core Facility for Protein X-ray Crystallography, Academia Sinica, Taipei 115, Taiwan

Octaprenyl pyrophosphate synthase (OPPs) catalyzes consecutive condensation reactions of farnesyl pyrophosphate (FPP) with isopentenyl pyrophosphate (IPP) to generate C_{40} octaprenyl pyrophosphate (OPP), which constitutes the side chain of bacterial ubiquinone or menaquinone. In this study, the first structure of long chain C_{40}-OPPs from *Thermotoga maritima* has been determined to 2.28-Å resolution. OPPs is composed entirely of α-helices joined by connecting loops and is arranged with nine core helices around a large central cavity. An elongated hydrophobic tunnel between D and F α-helices contains two DD*XX*D motifs on the top for substrate binding and is occupied at the bottom with two large residues Phe-52 and Phe-132. The products of the mutant F132A OPPs are predominantly C_{50}, longer than the C_{40} synthesized by the wild-type and F52A mutant OPPs, suggesting that Phe-132 is the key residue for determining the product chain length. Ala-76 and Ser-77 located close to the FPP binding site and Val-73 positioned further down the tunnel were individually mutated to larger amino acids. A76Y and S77F mainly produce C_{20} indicating that the mutated large residues in the vicinity of the FPP site limit the substrate chain elongation. Ala-76 is the fifth amino acid upstream from the first DD*XX*D motif on helix D of OPPs, and its corresponding amino acid in FPPs is Tyr. In contrast, V73Y mutation led to additional accumulation of C_{30} intermediate. The new structure of the *trans*-type OPPs, together with the recently determined *cis*-type UPPs, significantly extends our understanding on the biosynthesis of long chain polyprenyl molecules.

Prenyltransferases catalyze consecutive condensation reactions of isopentenyl pyrophosphate (IPP)[1] with allylic pyrophosphate to generate linear isoprenyl polymers (1–3). Starting from IPP and its isomer dimethylallyl pyrophosphate, the C_{15} farnesyl pyrophosphate (FPP) is formed by farnesyl pyrophosphate synthase (FPPs) (4). Using FPP and IPP as substrates, C_{40} octaprenyl pyrophosphate (OPP) is synthesized by octaprenyl pyrophosphate synthase (OPPs) via five IPP condensation reactions with FPP (5, 6). This polymer serves as the side chain of bacterial ubiquinone or menaquinone, a component involved in electron transfer for oxidative phosphorylation (7). Previously we have identified an OPPs from hyperthermophilic bacterium *Thermotoga maritima* (8). Compared with its mesophilic counterpart OPPs in *Escherichia coli* (9), the thermophilic enzymes shows higher product specificity, higher thermal stability, and lower structural flexibility.

During each IPP condensation, a new double bond is formed. Thus the prenyltransferases are classified as *cis*- and *trans*-type depending on the stereoisomer of the double bond formed (10). Two DD*XX*D motifs in the amino acid sequences were found in *trans*-type prenyltransferases. The first motif is responsible for binding with FPP, and the second motif is responsible for IPP binding (11–14). OPPs is a *trans*-type enzyme synthesizing the C_{40} long chain product. The only other *trans*-type enzyme with known structure is FPPs of the short chain type (15). Based on its three-dimensional structure and mutagenesis studies, a bulky amino acid residue located in the fifth position before the first DD*XX*D motif of FPPs appeared to block further elongation of the product FPP (16). The corresponding amino acid in OPPs is substituted with a small amino acid Ala (see Fig. 1), which may be required to remove the steric obstacle for OPPs to synthesize larger product than FPP. Further elongation is stopped by the large amino acids at the distal end of the active site to form the final C_{40} product.

In *cis*-type prenyltransferases, which catalyze long chain-length products in general, a large amino acid, Leu-137, located on the bottom of the tunnel-shaped active site, was concluded to provide a seal and thus to determine the final product chain length for undecaprenyl pyrophosphate synthase (UPPs) (17). The replacement of the Leu-137 with small Ala residue resulted in the synthesis of longer product C_{70} than C_{55} produced

* The synchrotron data collection was conducted with the Biological Crystallography Facilities (Taiwan Beamline BL12B2 at SPring-8) supported by the National Science Council (NSC). This work was supported in part by grants from Academia Sinica and National Science Council (NSC91-3112-P-001-019-Y) (to A. H.-J. W.). The costs of publication of this article were defrayed in part by the payment of page charges. This article must therefore be hereby marked "*advertisement*" in accordance with 18 U.S.C. Section 1734 solely to indicate this fact.

The atomic coordinates and structure factors (code 1V4E for native OPPs, 1V4H for F52A, 1V4J for V73Y, 1V4K for S77F, and 1V4I for F132A) have been deposited in the Protein Data Bank, Research Collaboratory for Structural Bioinformatics, Rutgers University, New Brunswick, NJ (http://www.rcsb.org/).

** To whom correspondence may be addressed: Inst. of Biological Chemistry, Academia Sinica, 128 Academia Rd., Taipei 115, Taiwan. Tel.: 886-2-2785-5696 (ext. 6070); Fax: 886-2-2788-9759; E-mail: phliang@gate.sinica.edu.tw.

‡‡ To whom correspondence may be addressed: Inst. of Biological Chemistry, Academia Sinica, 128 Academia Rd., Taipei 115, Taiwan. Tel.: 886-2-2788-1981; Fax: 886-2-2788-2043; E-mail: ahjwang@gate.sinica.edu.tw.

[1] The abbreviations used are: IPP, isopentenyl pyrophosphate; FPP, farnesyl pyrophosphate; FPPs, farnesyl pyrophosphate synthase; OPP, octaprenyl pyrophosphate; OPPs, octaprenyl pyrophosphate synthase; SPPs, solanesyl pyrophosphate synthase; DPPs, decaprenyl pyrophosphate synthase; GGPPs, geranylgeranyl pyrophosphate synthase; UPPs, undecaprenyl pyrophosphate synthase; TLC, thin layer chromatography.

TABLE I
Primers used to construct OPPs mutants in this study

Mutant name	Primer sequence
F52A	5′-GAGTGAGACTTTCGATACTTTCTGCCAAAAATAGAGGAGTAGAG-3′
F132A	5′-GGAAATAACAAACTGAGAAGAGCTGCTTTGAATGTGATCGGG-3′
V73Y	5′-CTTGCAGCTCTCGAACTCTATCACCTTGCCTCACTCCTCCAC-3′
A76Y	5′-CTCGAACTCGTTCACCTTTACTCACTCCTCCACGACGATGTG-3′
S77F	5′-CACATCGTCGTGGAGGAGAAAGGCAAGGTGAACGAGTTCGAG-3′
A76Y/S77F	5′-GCTCTCGAACTCGTTCACCTTTACTTTCTCCTCCACGACGATGTG-3′

TABLE II
Data collection and refinement statistics for wild-type, F52A, V73Y, S77F, and F132A OPPs
The unit cell dimensions for wild-type and V73Y ($P42_12$) are $a = b = 151.53$ and $c = 69.72$ Å (two molecules per asymmetric unit) and for F52A, S77F, and F132A (I422) are $a = b = 152.33$ and $c = 65.29$ Å (one molecule per asymmetric unit).

Data set	Wild-type	F52A	V73Y	S77F	F132A
Space group	$P42_12$	I422	$P42_12$	I422	I422
Resolution (Å)	2.28	2.80	2.85	2.45	2.40
No. of reflections					
Unique	36239	9680	18359	13817	14500
Observed	360254	89703	129154	123482	124260
Completeness (%)[a]	96.3 (95.8)	99.2 (100)	99.9 (100)	96.8 (82)	95.4 (81.7)
R_{merge} (%)[a]	5.9 (42.3)	5.6 (45)	7.0 (59.8)	5.3 (48.6)	4.2 (45.6)
$\upsilon/\sigma(I)$[a]	31.48 (4.36)	32.87 (4.27)	16.96 (3.57)	35.90 (2.90)	40.02 (2.55)
Refinement					
Resolution limits (Å)	50–2.28	50–2.80	50–2.85	50–2.45	50–2.40
R_{factor} (%)[a]	22.46 (26.33)	21.88 (27.93)	23.67 (30.88)	21.09 (23.16)	22.45 (27.13)
R_{free} (%)[a]	28.42 (31.76)	27.45 (34.16)	27.42 (30.26)	28.02 (29.89)	27.64 (28.28)
Deviations					
Bond lengths (Å)	0.0039	0.0037	0.0042	0.0047	0.0035
Bond angles (°)	1.103	0.965	0.997	1.163	0.900
Average B factors (Å^2)	46.50	52.79	53.37	43.43	49.60
Ramachandran plot					
Favored	92.8	91.5	92.4	91.5	91.6
Additionally allowed	6.4	7.7	6.8	7.3	7.6
Generously allowed	0.8	0.8	0.8	1.2	0.8
Disallowed	0	0	0	0	0

[a] The values in parentheses are for highest resolution shells.

by the wild-type enzyme. Near the substrate binding site on top of the tunnel, substitution of the small amino acid Ala-69 with a larger Leu led to the accumulation of C_{30} intermediate. This indicates that the space between Ala-69 and the FPP site allows the incorporation of three IPP, and the Leu at this position can temporarily block the chain elongation of this intermediate.

As reported herein, we have solved several crystal structures of OPPs from *T. maritima*. Interestingly, the structure of *T. maritima* OPPs bears a close resemblance to that of FPPs in which the molecule is entirely made of α-helices. The two DD*XX*D motifs are juxtapositioned around the active site in ways similar to those found in FPPs. At the bottom of its elongated active site cavity, two large Phe residues were mutated with smaller Ala to test their roles in determining the final product chain length. Near the top of the tunnel, three amino acids, Val-73, Aala-76, and Ser-77, were substituted with larger ones to probe the FPP binding site. Our results provide further insights into the catalytic mechanism of the *trans*-type prenyltransferases.

EXPERIMENTAL PROCEDURES

Materials—Radiolabeled [^{14}C]IPP (55 mCi/mmol) was purchased from Amersham Biosciences, and FPP was obtained from Sigma. Reverse-phase thin layer chromatography (TLC) plates were purchased from Merck. PfuTurbo DNA polymerase was obtained from Invitrogen. The plasmid mini-prep kit, DNA gel extraction kit, and nickel-nitrilotriacetic acid resin were purchased from Qiagen. Potato acid phosphatase (2 units/mg) was purchased from Roche Applied Science. FXa and the protein expression kit (including the pET32Xa/LIC vector and competent JM109 and BL21 cells) were obtained from Novagen. The QuikChange site-directed mutagenesis kit was obtained from Stratagene. All commercial buffers and reagents were of the highest grade.

Site-directed Mutagenesis of OPPs—OPPs mutants were prepared by using QuikChange site-directed mutagenesis kit in conjunction with the *Thermotoga* OPPSs gene template in the pET32Xa/Lic vector. The mutagenic primers used were prepared by Biobasic, Inc. (Canada). The mutagenic oligonucleotides for performing site-directed mutagenesis are listed in Table I. The basic procedure of mutagenesis utilizes a supercoiled double-stranded DNA vector with an insert of interest and two synthetic oligonucleotide primers containing the desired mutation. The mutation was confirmed by sequencing the entire OPPs mutant gene of the plasmid obtained from the overnight culture. The correct construct was subsequently transformed to *E. coli* BL21 (DE3) for protein expression. The procedure for protein purification followed our reported protocol (8). Each purified mutant OPPs was verified by mass spectroscopic analysis, and its purity (>95%) was checked by SDS-PAGE.

Crystallization and Data Collection—Wild-type OPPs and four mutants including F52A, F132A, V73Y, and S77F were crystallized using the hanging drop method from Hampton Research (Laguna Niguel, CA) by mixing 2 μl of the OPPs solution (10 mg/ml in 0.1% Triton X-100) with 2 μl of the mother liquor (0.1 M Na^+Hepes, pH 7.5, and 1.5 M $LiSO_4$), equilibrating with 500 μl of the mother liquor. Within 4 days, crystals had grown to dimensions of about 0.4 × 0.4 × 0.2 mm. The x-ray diffraction data sets for the wild-type OPPs, F52A, V73Y, S77F, and F132A were collected to 2.28-, 2.85-, 2.85-, 2.45-, and 2.4-Å resolution, respectively. OPPs mutants and multiple isomorphous replacement data sets were collected in house using a Rigaku MicroMax002 x-ray generator equipped with R-Axis IV^{2+} image plate detector. The wild-type OPPs x-ray diffraction data set was collected at 100K on the Taiwan Contract BL12B2 stations at SPring-8 (Hyogo, Japan).

OPPs wild-type and V73Y mutant crystals belong to the tetragonal space group $P42_12$ with the following unit cell parameters: $a = b = 151.53$ and $c = 69.72$ Å. F52A, S77F, and F132A mutants belong to the tetragonal space group I422 with the following unit cell parameters: $a = b = 152.31$ and $c = 65.38$ Å. All diffraction measurements were carried out on crystals cryoprotected with 0.1 M Na^+Hepes buffer, pH 7.5, and 2.5 M Li_2SO_4.

Structure Determination and Refinement—For wild-type OPPs, three mercury data sets were used for phase calculation by the multiple

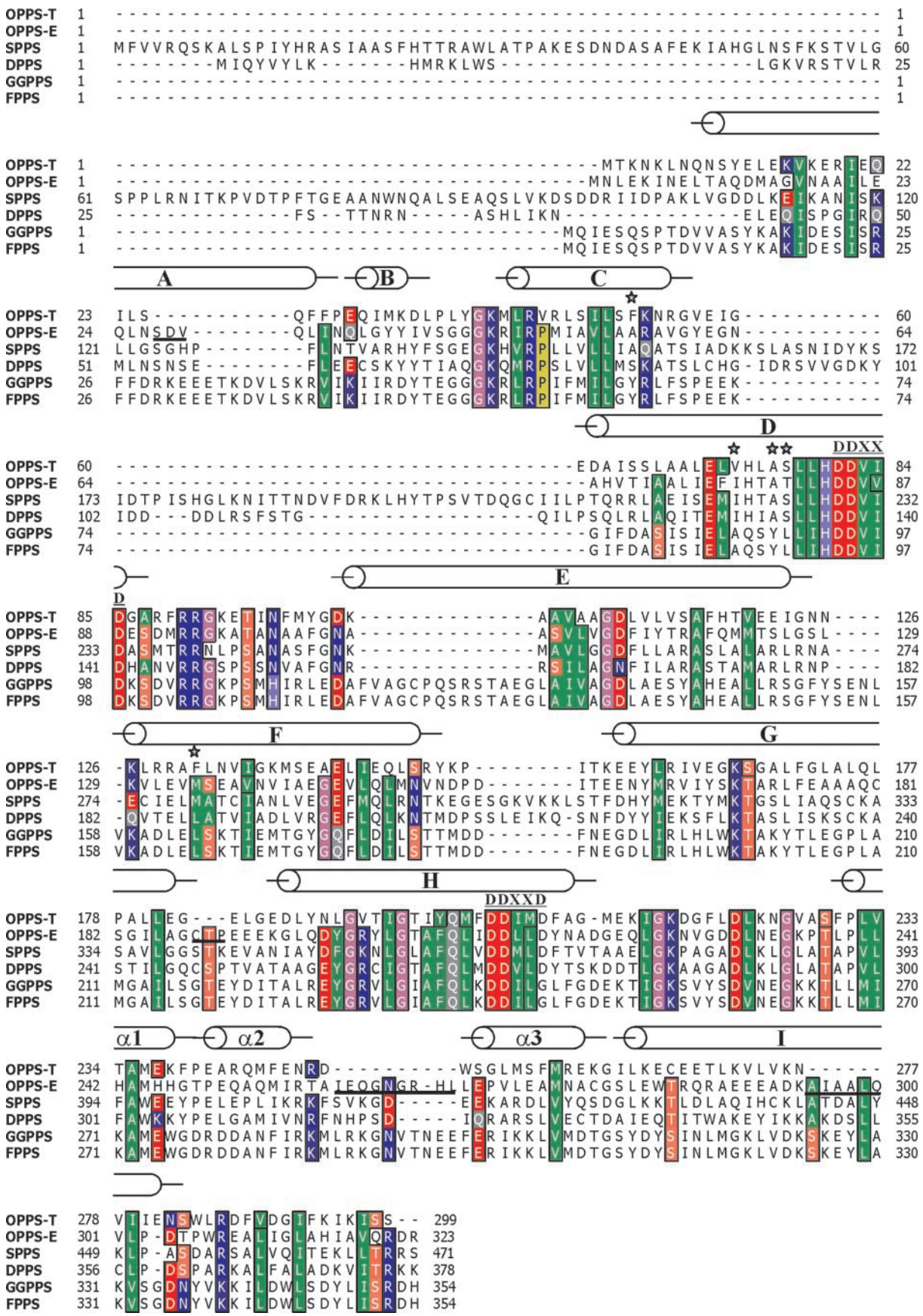

FIG. 1. **Alignment of amino acid sequences of the *T. maritima* OPPs, *E. coli* OPPs, *Mucor* C_{45}-SPPs, fission yeast C_{50}-DPPs, *Thermoplasma* C_{20}-GGPPs, and *Thermoplasma* FPPs.** *Colored outlines* indicate identical and similar amino acid residues, respectively. The *stars* indicate the amino acid residues mutated in this study. The *underlined* are the extra sequences of *E. coli* OPPs compared with *T. maritima* OPPs. Ala-76 in OPPs corresponds to the large Tyr-89 and Tyr-89 in short chain GGPPs and FPPs, respectively.

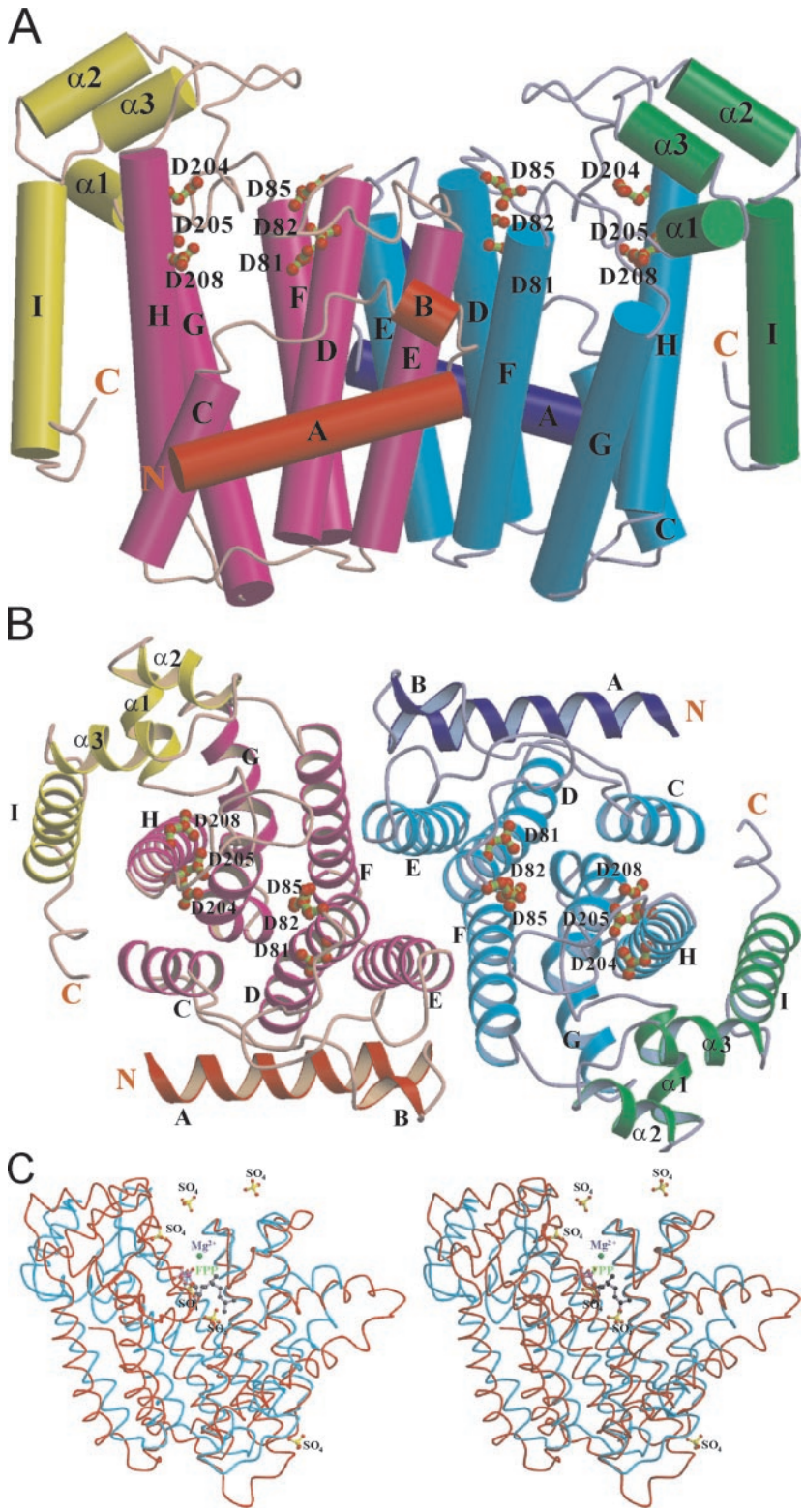

FIG. 2. *A*, the side view model of *T. maritima* OPPs is shown using a cylinder diagram. Two identical subunits are associated into a dimer by forming a four-layer helix bundle. The N-terminal α helical hairpins in the outer layers are shown in *blue* and *red* for the two individual subunits, whereas the eight helices in the inner layers are shown in *cyan* and *magenta*. Two small peripheral domains are colored *green* and *yellow*. *Black arrows* indicate the location of the active site with the Asp residues in the two DD*XX*D motifs shown in *red*. In *B*, the top view model of *T. maritima* OPPs is shown using a ribbon diagram. The color and styles shown here are the same as above. In *C*, two homologous proteins, avian FPPs (in *green*) including FPP and Mg^{2+} ion and *T. maritima* OPPs (in *red*) containing six sulfate ions, are superimposed by SPDB viewer (27). The FPP, Mg^{2+} ion, and six sulfate ions observed in OPPs structure are shown with ball-and-stick model. FPP and sulfate are shown in *black* and *yellow*, respectively. These figures are produced using MolScript (28) and Raster3D (29).

isomorphous replacement method using SOLVE (18). The phases of wild-type OPPs structure were solved using $CH_3HgOOCCH_3$, $Hg(CN)_2$, and $C(HgOOCH_3)_4$ heavy atoms as reported previously (19). The phases of OPPs mutants (F52A, V73Y, S77F, F132A) were solved by the molecular replacement method using the program CNS (20). Refinement statistics of collected data for these OPPs are summarized in Table II.

Kinetic Parameters for Mutant OPPs—For enzyme activity measurements, mutant OPPs enzymes (0.1 μM F52A, V73Y, A76Y, S77F, A76Y/S77F, and F132A) were used. The reaction was initiated in 200-μl solution containing 100 mM Hepes, pH 7.5, 5 μM FPP, 50 μM [^{14}C]IPP, 50 mM KCl, and 0.5 mM $MgCl_2$ at 25 °C. The enzyme concentration used in all experiments was determined from its absorbance at 280 nm (ϵ = 20,340 M^{-1} cm^{-1}). The reaction was terminated by adding 10 mM (final concentration) EDTA, and the product was extracted with 1-butanol. The product was quantitated by counting the radioactivity in butanol phase ([^{14}C]IPP in aqueous phase) using a Beckman LS6500 scintillation counter. The OPPs mutants' steady-state k_{cat} was calculated based on the rate of IPP consumption.

Single-turnover Experiments of V73Y—The single-turnover reaction was initiated by mixing 15 μl of V73Y (10 μM) preincubated with FPP (2 μM) with equal volume of [^{14}C]IPP (50 μM) solution in buffer containing 100 mM Hepes, pH 7.5, 0.5 mM $MgCl_2$, and 50 mM KCl at 25 °C. The concentrations cited in parentheses and hereafter in the paper are those after mixing. The reaction mixture quenched with EDTA in the speci-

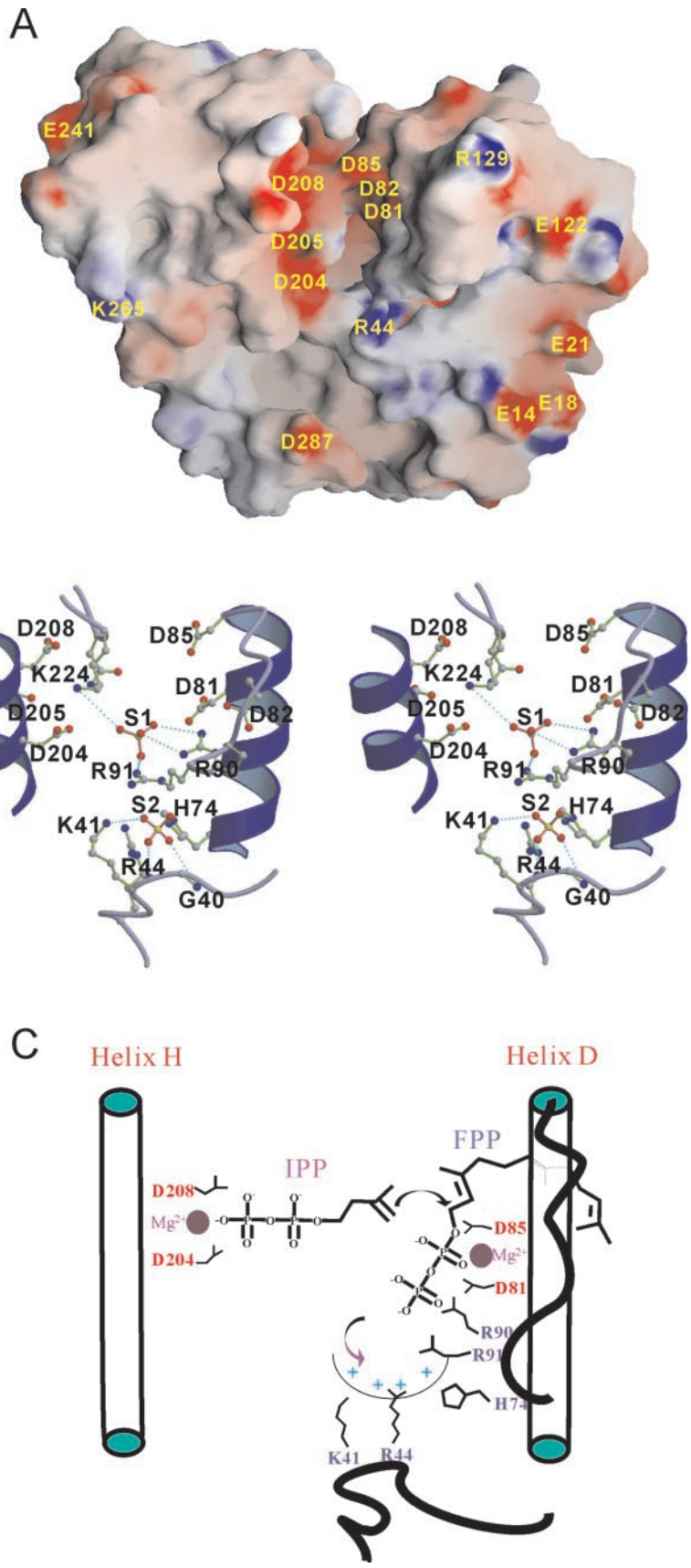

FIG. 3. **OPPs active site structure and reaction mechanism.** In *A*, the surface of active site is color coded from *red* to *blue* according to charge potential from −15 to 15 k_BT. This figure was generated using GRASP (30). In *B*, two sulfate ions in the active site of totally six sulfates of OPPs F132A mutant are shown (these sulfate ions are more obvious than other data sets). Along with two sulfate ions, amino acids Lys-41, Arg-44, His-74, Asp-81, Asp-82, Asp-85, Arg-90, Arg-91, Asp-204, Asp-205, and Asp-208 are shown in ball-and-stick model. S1 containing the first DD*XX*D motif is responsible for binding with FPP, and S2 located downstream the FPP binding site functions to stabilize the PP_i leaving group. This is illustrated in *C* that Arg-90 and Arg-91 are important in FPP binding, and AArg-44, Lys-41, and His-74 surround another sulfate ion to grasp the leaving group of FPP while reaction occurs.

fied time period was extracted with the same volume of 1-butanol, and the radioactivity in the organic phase (intermediates and product) was counted by the scintillation counter (Beckman LS6500).

Product Analysis—The OPPs reaction containing 1 μM enzyme (wild-type and mutant OPPs), 50 μM [^{14}C]IPP, 5 μM FPP, 0.1% Triton X-100, 0.5 mM $MgCl_2$, and 50 mM KCl in 100 mM Hepes buffer, pH 7.5, was performed for 72 h at 25 °C. The 10 mM EDTA was used to terminate the reactions. The radiolabeled polyprenyl pyrophosphate products were extracted with 1-butanol. The 1-butanol was then evaporated, and the 20% propanol solution containing 4.4 units/ml acidic phosphatase,

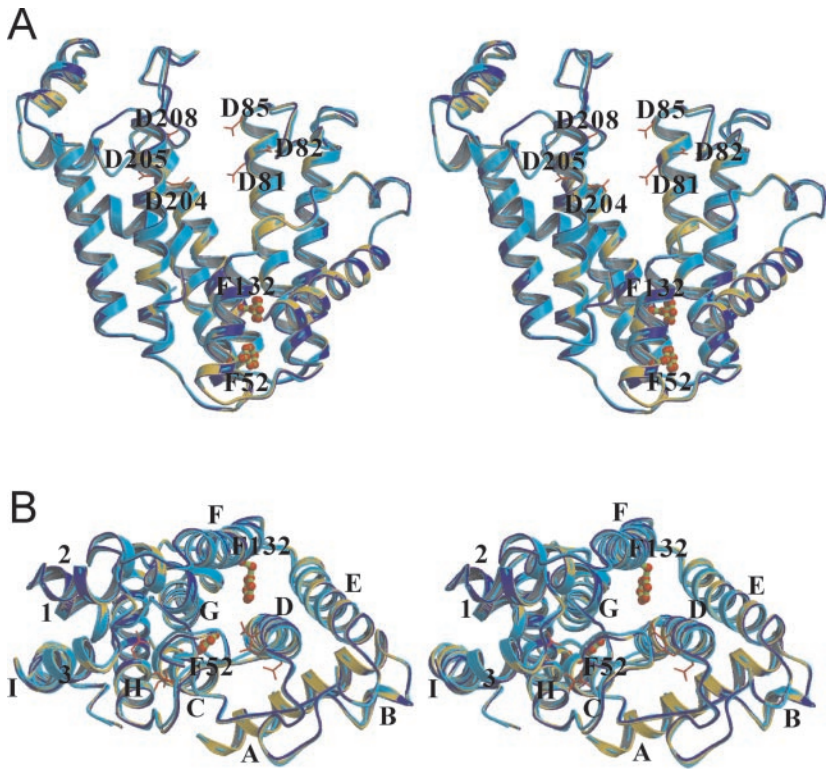

FIG. 4. **F132 determines the chain length of final product.** The side view (*A*) and top view (*B*) of the Phe-132 and Phe-52 residues in one monomer wild-type OPPs superimposed with F132A and F52A structures are shown using a ribbon diagram. Wild-type OPPs, F132A, and F52A are shown in *blue*, *cyan*, and *yellow*. Phe-132 is located on the bottom of the tunnel as a floor surrounded by helices D and F. Phe-52, on the other hand, is located in another place (bottom of helix C) of the structure.

0.1% Triton, 50 mM sodium acetate, pH 4.7, was prepared to convert polyprenyl pyrophosphate products to corresponding alcohols according to the reported procedure (21). After the pyrophosphate hydrolysis catalyzed by acidic phosphatase was completed, the polyprenols were extracted with *n*-hexane. The hexane volume was reduced by evaporation. The polyprenols were separated on reversed-phase TLC using acetone/water (19:1) as mobile phase. The radiolabeled products were identified by autoradiography using a bioimaging analyzer FUJIFILM BAS-1500 (Japan) according to their R_f values reported. The percentages of the intermediates and product formed in the OPPs reaction were calculated from the measured intensities normalized by the numbers of [^{14}C]IPP incorporated.

TABLE III
Steady-state activities of T. maritima OPPs (wild-type and mutants) assayed under 5 μM FPP and 50 μM [^{14}C]IPP at pH 7.5 and 25 °C

T. maritima OPPs	Steady-state activity (s^{-1})
Wild-type	5×10^{-3}[a]
V73Y	3.3×10^{-3}
A76Y	7.3×10^{-5}
S77F	2.91×10^{-7}
A76Y/S77F	2.26×10^{-7}
F52A	3.53×10^{-3}
F132A	5.09×10^{-3}

[a] The number is adopted from Ref. 8.

RESULTS

Comparison of Amino Acid Sequences of trans-Prenyltransferases—In Fig. 1, the amino acid sequences of several *trans*-prenyltransferases including C_{40}-OPPs from *T. maritima* and *E. coli*, C_{45}-solanesyl pyrophosphate synthase (SPPs) from *Mucor*, C_{50}-decaprenyl pyrophosphate (DPPs) from fission yeast, C_{20}-geranylgeranyl pyrophosphate synthase (GGPPs), and C_{15}-FPPs from *Thermoplasma* are aligned. They all contain two DD*XX*D motifs for FPP and IPP binding enzyme and reaction. *T. maritima* OPPs and *Thermoplasma* FPPs are of 20% sequence identity and 46% similarity. The amino acid located in the fifth position before the first DD*XX*D is a small alanine in *T. maritima* OPPs, *E. coli* OPPs, SPPs, and DPPs. On the other hand, GGPPs and FPPs have a large Tyr at this position, suggesting that this residue is important in determining the chain length of the product. As shown below, the A76Y mutant of *T. maritima* OPPs indeed has altered the product from C_{40} to C_{20}. The roles of nearby amino acids Ser-77 and Val-73 in affecting product chain length were also examined. The two phenylalanines, Phe-132 and Phe-52, were tested by site-directed mutagenesis for their function in determining the ultimate chain length of the product. The mutated residues studied here are indicated by *stars* in Fig. 1.

Compared with the amino acid sequence of thermophilic *T. maritima* OPPs, mesophilic *E. coli* enzyme has four extra short sequences as shown by underlines in its amino acid sequence (Fig. 1). The first and the last extra short sequences are located in the helix A and I, respectively, whereas others are in the loop regions. These extra sequences are not close to the active site but may play a structural role in providing *E. coli* OPPs with flexibility. The *T. maritima* OPPs without these sequences is more rigid (8).

Overall Structure—In the present studies, we have solved the crystal structures for wild-type, F52A, V73Y, S77F, and F132A OPPs. Wild-type and V73Y OPPs belong to $P42_12$ space group. Each asymmetric unit of the crystal unit cell contains one OPPs dimer, which is the active form of the enzyme. Two identical subunits are associated into a dimer by forming a four-layer helix bundle using helices E and F (Fig. 2, *A* and *B*). F52A, S77F, and F132A OPPs belong to I422 space group. A crystallographic 2-fold symmetry lies in the center of the dimer and each asymmetric unit of the crystal unit cell contains only one OPPs monomer. The refined structure of wild-type OPPs in complex with six sulfate ions contains amino acid residues 9–288 in two subunits. The structure contains 12 α-helices, nine of them surrounding a large central cavity (helix A to I). Two conserved DD*XX*D sequences are located on helices D and H near the opening of this deep cleft of the substrate binding pocket. Between helix H and I are three short α-helices, with helix α1 (Pro-231-Lys-238), α2 (Glu-241-Glu-247), α3 (Ser-252-Glu-260) on the outer surface of the α-cone. These three α helices (α1, α2, and α3) interact with two loops (loop1 between F and G as well as loop2 between H and α1) by hydrophobic

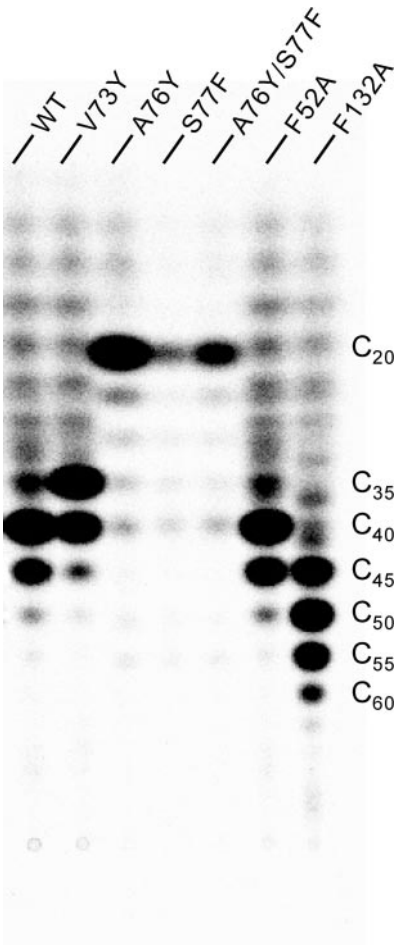

FIG. 5. **The products synthesized by V73Y, A76Y, S77F, A76Y/S77F, F52A, and F132A.** The reaction mixture containing 0.5 μM each mutant enzyme, 5 μM FPP, and 50 μM [^{14}C]IPP was incubated at 25 °C for 100 h to complete the reaction. The final products were extracted and analyzed using TLC and phosphorimaging. A76Y synthesizes shorter product C_{20}, and F132A generated longer product (major product = C_{50}) than the C_{40} synthesized by wild-type.

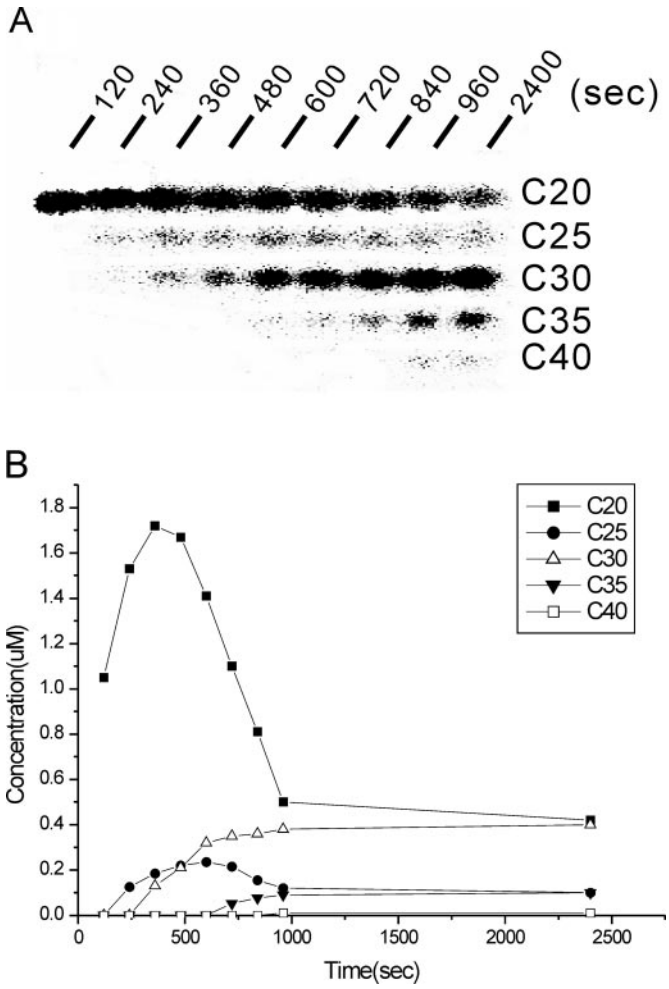

FIG. 6. **Single-turnover intermediate time course of V73Y.** In the reaction at 25 °C, 10 μM mutant enzyme, 2 μM FPP, and 50 μM [^{14}C]IPP were used. The reaction was terminated after specified reaction time, and the intermediates formed at each time point were analyzed using TLC as shown in *A*. A quantitative expression (*B*) of the image data is also presented (C_{20}, ■), C_{25} (●), C_{30} (△), C_{35} (▼), and C_{40} (□)). In *A* for the single-turnover reaction of V73Y, accumulation of C_{20} and C_{30} to a greater extent and longer time compared with the other intermediates were observed.

interactions provided by amino acids Tyr-151, Pro-153, Tyr-159, Phe-209, Phe-220, Phe-230, Pro-231, Phe-239, Phe-246, Trp-251, and Phe-257. Although helices α1, α2 and α3 are not directly involved in the structure of active site, it may pull loop2 to keep the top of the active site tunnel open and allow the IPP and FPP substrates to enter the tunnel.

Helices E and F are involved in the dimer formation with the major stabilization coming from the helices E(a chain)–E(b chain) and E(a chain)-F(b chain) inter-subunit hydrophobic interactions and hydrogen bonding. The side-chain of Phe-117 is stacked with that of Phe-117 from the other subunit.

Comparison of Thermotoga OPPs Structure with Avian FPPs—OPPs shares the same folding as avian FPPs (Fig. 2*C*), although OPPs and avian FPPs only have 16% sequence identity and 38% similarity. OPPs and FPPs are superimposed better in helices C, D, E, F, and G with root mean square deviation = 2.54 Å for the fitting of 332 Cα atoms of the dimer OPPs. However, helix B, the loop between helices A and B and the loop between helices C and D of OPPs are shorter than that of FPPs. This probably results in a more rigid structure of the thermophilic OPPs. The plane formed by helices H, α1, α2, α3, I and J are slightly rotated by 5–10 degrees relative to each other in comparing the two structures. In OPPs, the electron density map for residues 289–299 at the C-terminal end is not visible. Notably, the loops on the top of helices F-H are pulled by hydrophobic interaction provided by several hydrophobic residues and kept away from the opening for substrate entrance between helices D and F.

Active Site Location—An elongated tunnel-shaped cavity surrounded by four α-helices (helices C, D, F, and H) can be proposed as the active site, because the two DD*XX*D motifs for substrate binding are located in helix D and H, respectively, near the top of the tunnel (Fig. 2*A*). Hydrophobic side chains of the amino acids cover the entire inner surface of the tunnel, except near the two DD*XX*D conserve motifs for substrate binding. The amino acids in the region of substrate binding site are displayed in Fig. 3*A*. Two sulfate ions were found in the active sites of both mutant and wild-type OPPs structures, but F132A OPPs had the most obvious electronic density for these sulfate ions. F132A OPPs structure was therefore used to show the substrate binding site of OPPs (Fig. 3*A*). The A, B subunits of the wild-type and V73Y OPPs are superimposed well with F52A, S77F, and F132A (data not shown). Six sulfates appear in each subunit of OPPs. Two sulfate ions, called S1 and S2, are directly attached to the two DD*XX*D via Mg^{2+}, respectively, which resemble the pyrophosphate moiety of the substrates. Two of these sulfate ions, S3 and S4, are located in the outer face of the tunnel. S3 is hydrogen bonded to the nitrogen atoms of Arg-150 and S4 forms hydrogen bonds with backbone hydro-

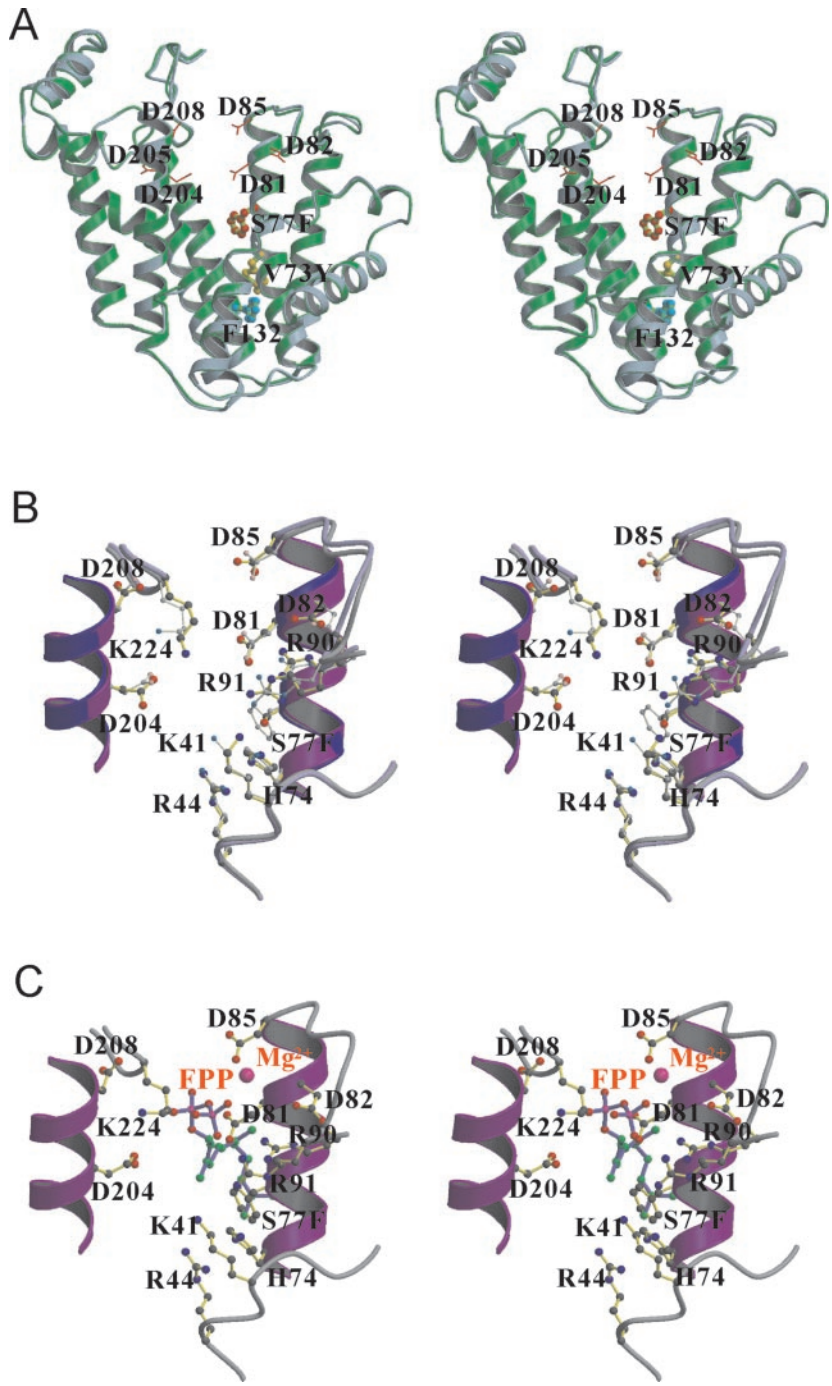

FIG. 7. **The structures of S77F and V73Y mutants.** The side view (*A*) of the S77F structure superimposed with V73Y structure is shown using a ribbon diagram. S77F and V73Y structures are shown in *green* and *light blue*, the S77F, V73Y and Phe-132 residues are shown in *red*, *yellow*, and *green*, respectively. The mutated residues in OPPs affect FPP chain elongation. Based on V73Y structure, V73Y is located upstream from Phe-132 by 5.83 Å, so V73Y can produce C_{30}, two IPP units shorter from OPP. In *B*, the active site of wild-type OPPs is superimposed with S77F mutant structure. Wild-type OPPs and S77F structures are shown in *blue* and *magenta*, and the residues of S77F structure are shown in a delicate shade and smaller atoms. In *C*, the active site of S77F structure is modeled with Mg^{2+} ion and FPP. Mg^{2+} is shown in *pink*, and the pyrophosphate moiety of FPP is shown in *red*. S77F protrudes into the bottom of FPP binding site. Therefore, the mutant only synthesizes C_{20} product.

gens of Glu-146, Leu-148, and the side chain nitrogen atoms of Gln-147. It appears that these amino acid residues may initially attract the substrates to aid their binding in the active site.

Around the active site, polar (mostly positively charged) residues including Arg-90, Arg-91, His-74, Lys-41, and Arg-44 surround the pyrophosphate portion of FPP (Fig. 3*B*). The distance between two side chains of the Asp residues (Asp-85 and Asp-208) in DD*XX*D motifs of helices D and H is ~11 Å. Further down, the funnel diameter near the bottom of the hydrophobic tunnel, occupied by Phe-132, narrows down to ~3 Å. The distance between the conserved DD*XX*D and Phe-132 is ~24 Å, sufficiently long for accommodating C_{40}-prenyl chain. Based on our structure, Phe-52 is putative "floor" for the active site tunnel depending on which way the FPP chain elongation is directed. To test the role of Phe-132 and Phe-52 in sealing the bottom of the tunnel, the mutants F132A and F52A were prepared, and their products were examined as shown below.

Products Generated by F52A and F132A—The structure of *T. maritima* OPPs reveals a hydrophobic tunnel formed mostly by helices D and H. Two DD*XX*D motifs located on top of the tunnel facing each other likely represent the FPP and IPP binding site, respectively. As mentioned above, two large amino acid residues, Phe-52 and Phe-132, occupy the bottom portion of the tunnel (Fig. 4, *A* and *B*). One of these residues or both may provide the blockage for further chain elongation of C_{40} product, analogous to Leu-137 in sealing the bottom of UPPs active site (17). We replaced these large residues with Ala and examined the chain lengths of the products synthesized by the mutant enzymes by TLC analysis. Both mutant enzymes F52A and F132A have similar activity compared with the wild-type (see Table III). The final products of wild-type and mutant

enzymes under 5 μM FPP and 50 μM [^{14}C]IPP were obtained in 100 h because of the low activity of *T. maritima* OPPs. As shown in Fig. 5, under the same reaction condition, F52A generated products similar to that of the wild-type OPPs (C_{35}:C_{40}:C_{45} = 6:83:11 for wild-type and C_{35}:C_{40}:C_{45} = 6:76:18 for F52A). In contrast, F132A synthesized longer products (C_{40}:C_{45}:C_{50}:C_{55}:C_{60} = 2:27:49:19:3). Apparently, Phe-132 rather than Phe-52 plays a critical role in product chain length determination.

We hypothesize that the substitution of the large Phe-132 with a smaller in Ala removes the floor of the tunnel, thereby allowing for the formation of longer chain-length products. The wild-type OPPs structure is superimposed very well with the F132A and F52A structures (Fig. 4, *A* and *B*). From the crystal structure, the side chain of Phe-132 is pointed toward the tunnel interior (Fig. 4*A*, *side view*). From the top view (Fig. 4*B*), Phe-132 is well positioned to seal the bottom of the hollow tunnel. On the other hand, Phe-52 is located on the other side of the tunnel, and Phe-52 cannot block the bottom of the tunnel. (Fig. 4*A*, *side view*). Because the F132A and F52A are structurally the same as the wild-type enzyme except for the change in the side chain, we thus identify the single residue for determining the ultimate chain length of OPPs product. This also clearly shows that the chain elongation of FPP in OPPs reaction is along one side (helix D) of the tunnel.

Products of V73Y, A76Y, S77F, and A76Y/S77F—Near where the substrates FPP and IPP bind, several amino acids including Val-73, Aala-76, and Ser-77 are found. Among them, Ala-76 is a small amino acid and is located in the fifth position upstream from the first DD*XX*D motif in OPPs sequence (see Fig. 1). The corresponding residue at this position for FPPs from *Bacillus stearothermophilus* is a large Tyr, and when changed to smaller residue such as Gly and Ala the product chain length was increased the most (22, 23). In addition to the fifth amino acid residue, sixth and eighth positions before the first DD*XX*D have also been shown important to control the product specificity of archael FPPs and C_{20}-GGPPs (24). In *T. maritima* OPPs, Ser-77, Ala-76, and Val-73 are located at the fourth, fifth, and eighth positions before the DD*XX*D motif, the predicted FPP binding site. In the active site tunnel, they are below, but still in close proximity to, the first DD*XX*D motif. By substituting these residues with larger ones, we generated S77F, A76Y, and V73Y mutants. Their main products are C_{35} for V73Y (C_{35}:C_{40} = 64:36), C_{20} for A76Y, S77F, and double mutant A76Y/S77F (Fig. 5). V73Y has similar activity to that of the wild-type whereas A76Y, S77F, and the double mutant have much lower activity (see Table III). This is because of the poor substrate binding and/or the alteration of active site conformation by the mutation. Comparison the active site of wild-type OPPs and S77F structure (see Fig. 7*B*), there are slight shift in the residue Lys-41, Arg-44, Arg-90, and Arg-91. The main chains of wild-type OPPs and S77F structure are superimposed well. The active site of OPPs is superimposed better with avian FPPs than whole structure. The active site of S77F structure is superimposed with avian FPPs, which was complex with Mg^{2+} and FPP. The active site model of S77F structure with Mg^{2+} and FPP is proposed (see Fig. 7*C*). Anyway, it is not surprising that these mutants generate C_{20} as final product, because Ala-76 and Ser-77 are located near the FPP site so their mutations to the large amino acids interfere with the chain elongation of substrate FPP (see Fig. 7, *A–C* for their structures). On the other hand, Val-73 is located further down the tunnel and away from the FPP site, so V73Y has final products more similar to that of the wild-type.

Intermediates of V73Y under Single-turnover Condition—Although the major product of V73Y has only one IPP unit shorter than the wild-type, we examined the intermediates in the V73Y reaction under single turnover at increased enzyme concentration to maximize the possibility of trapping transiently accumulated intermediate, which should reflect the altered size of active site caused by the mutation. The intermediates were trapped mostly at C_{20} and C_{30} (Fig. 6). Accumulation of C_{20} intermediate may result from the changed conformation of active site pocket, so only the bound IPP condenses with FPP to form C_{20}. On the other hand, C_{30} is accumulated to a greater extent compared with C_{25} and C_{35} intermediates, because V73Y interferes with proper binding of C_{30} and longer polymers. Val-73 is located on the top of Phe-132, and the 5.83-Å distance between two amino acids approximately can accommodate two IPP units (Fig. 7). Therefore, the substitution of Val-73 with a larger Tyr can partially block the tunnel and cause temporary accumulation of C_{30}.

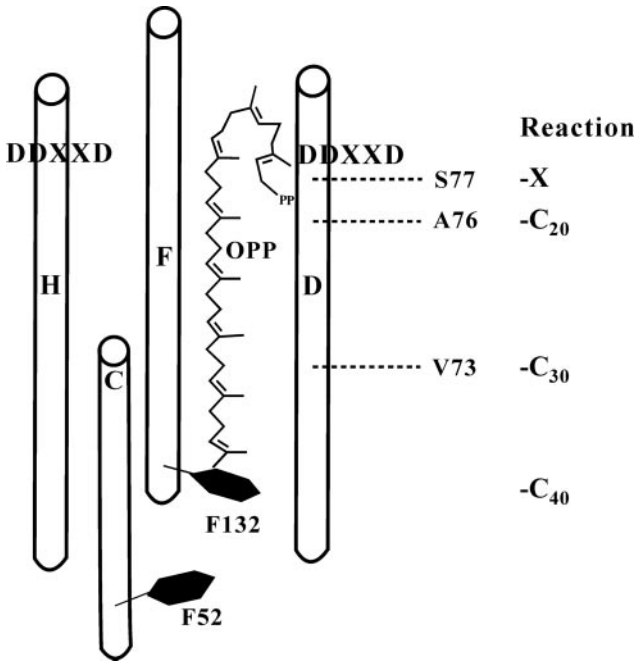

FIG. 8. **Proposed mechanism for chain length determination catalyzed by OPPs.** The first DD*XX*D motif attached to helix D represents the FPP binding site. Ser-77 and Ala-76 are located in immediate proximity of FPP, and V73Y is further down. The substitution of Ser-77 and Ala-76 with larger residues led to the formation of C_{20}, a single condensation between the bound FPP and IPP. V73Y mutation results in temporary accumulation of C_{30}. Phe-132 located on the bottom of helix D blocks further chain elongation of OPP and determines the ultimate product chain length.

DISCUSSION

The deduced amino acid sequences of several *trans*-prenyltransferases (Fig. 1) show amino acid sequence homology and two common DD*XX*D motifs among them (25). These Asp-rich motifs were recognized from the three-dimensional structure of FPPs and site-directed mutagenesis studies to be involved in substrate binding and catalysis via chelation with Mg^{2+}, a cofactor required for the enzyme activity. The three-dimensional structure of OPPs has a similar fold to the structure of FPPs. Two DD*XX*D motifs are located in the D and H helix, respectively, facing each other to create an active site for the binding of FPP and IPP. Site-directed mutagenesis studies have shown the importance of these Asp residues in substrate binding and catalysis (11–14). Besides the DD*XX*D, Arg-112 and Arg-113 of rat FPPs, as well as Arg-109 and Arg-110 of yeast FPPs (corresponding to Arg-90 and Arg-91, respectively, in *T. maritima* OPPs), had been identified essential for enzyme catalysis (12, 14). As illustrated in Fig. 3*C*, these positively

charged residues may facilitate the reaction by stabilizing the pyrophosphate leaving group.

The product specificity of FPPs can be modified to synthesize larger products by substituting Tyr-81 with smaller residues. Apparently, this residue located at the fifth position before the first DD*XX*D motif is the key residue in determining the product chain length for FPPs. Predicted from the structure of FPPs, this residue is located from the first Asp-rich motif at a distance of ~12 Å which is similar to the length of hydrocarbon moiety of FPP (23). The chain length of the product catalyzed by these mutants is inversely proportional to the accessible surface volume of the substituted amino acid residue in the first DD*XX*D. For OPPs, the fifth amino acid upstream from the first DD*XX*D (FPP site) is the small Ala (Ala-76). We have changed it to Tyr and found that the mutant enzyme generated C_{20} product. Ala-76 is located near the DD*XX*D and hampers the chain elongation of FPP. Therefore, only a single condensation occurs with the bound IPP, and the reaction rate for the mutant is 100-fold smaller than the wild-type.

Beside the C_{20} intermediate, C_{30} was also accumulated to a larger extent for V73Y. This residue is further down the tunnel, and its mutation to larger Tyr is predicted to interfere with the proper chain elongation of C_{30}. This mutant has a comparable rate constant to that of the wild-type, because the residue is more distant from the FPP binding site than Ala-76. On the other hand, Ser-77 is closer to the substrate site, and the mutant S77F has 10^4 lower activity than the wild-type. Its final product is also C_{20}, the same as A76Y, but the mutation significantly affects the binding of substrate and/or the active site conformation for catalysis (K_m of the substrate was not measured because of its extremely low activity).

Previously, A79Y mutant of *E. coli* OPPs was prepared and found completely inactive although the *E. coli* cells harboring wild-type *ispB* (gene encoding for OPPs in *E. coli*) and the A79Y mutant produced ubiquinone with C_{30} side chain. The mutant protein forms a heterodimer of His-tagged wild-type IspB and glutathione *S*-transferase-tagged A79Y. It was concluded that A79Y is functionally inactive, but it can regulate activity upon forming a heterodimer with wild-type OPPs, and this dimer formation is important for the determination of the isoprenoid length (26). However, from our studies, *T. maritima* OPPs mutant A76Y (a residue corresponding to Ala-79 in *E. coli* OPPs) has residual activity and produced C_{20} as major product.

Phe-132 represents the floor of the active site tunnel of OPPs based on the larger major product C_{50} synthesized by mutant F132A than C_{40} of the wild-type. In contrast, Phe-52, the other possible candidate for the floor, did not synthesize larger product when mutated to Ala. The longer products synthesized by F132A can be then blocked by residues Leu-128, Ile-123, and Asp-62 beneath the end of the tunnel. Apparently, the chain elongation of FPP is along the D helix. From the top view of this tunnel, Phe-132 can seal the bottom to block the additional chain elongation of the final product.

The corresponding residues in *E. coli* OPPs and *Mucor* C_{45}-SPPs to *T. maritima* OPPs Phe-132 residue are Met-135 and Met-279, respectively. The chain length may be determined by Met in *E. coli* OPPs (C_{40}) and *Mucor* SPPs (C_{45}).

The site-directed mutagenesis studies, combined with the three-dimensional structure presented here, provide a model (Fig. 8) for OPPs catalysis, substrate binding, and mechanism for product chain length determination. According to this model, FPP and IPP are bound with its PP_i group near the first and second DD*XX*D motif, respectively, with the help of Mg^{2+} ions. The C_{15}-FPP undergoes chain elongation with the incoming IPP toward the bottom of the tunnel sealed by Phe-132. The final C_{40} product is released from the top of the tunnel.

REFERENCES

1. Kellogg, B. A., and Poulter, C. D. (1997) *Curr. Opin. Chem. Biol.* **1,** 570–578
2. Ogura, K., Koyama, T., and Sagami, H. (1997) *Subcellular Biochem.* **28,** 57–87
3. Liang, P. H., Ko, T. P., and Wang, A. H.-J. (2002) *Eur. J. Biochem.* **269,** 3339–3354
4. Glomset, J. A., Gelb, M. H., and Farnworth, C. C. (1990) *Trends Biochem. Sci.* **15,** 139–142
5. Fujisaki, S., Nishino, T., and Katsuki, H. (1986) *J. Biochem.* (*Tokyo*) **99,** 1327–1337
6. Asai, K.-I., Fujisaki, Y., Nishimura, T., Nishino, T., Okada, K., Nakagawa, T., Kawamukai, H., and Matsuda, H. (1994) *Biochem. Biophys. Res. Commun.* **202,** 340–345
7. Soballe, B., and Poole, R. K. (1999) *Microbiology* **145,** 1817–1830
8. Kuo, T. H., and Liang, P. H. (2002) *Biochim. Biophys. Acta* **1599,** 125–133
9. Pan, J. J., Kuo, T. H., Chen, Y. K., Yang, L. W., and Liang, P. H. (2002) *Biochim. Biophys. Acta* **1594,** 64–73
10. Ogura, K., and Koyama, T. (1998) *Chem. Rev.* **98,** 1263–1276
11. Marrero, P. F., Poulter, C. D., and Edwards, P. A. (1992) *J. Biol. Chem.* **267,** 21873–21878
12. Joly, A., and Edwards, P. A. (1993) *J. Biol. Chem.* **268,** 26983–26989
13. Koyama, T., Tajima, M., Sano, H., Doi, T., Koike-Takeshita, A., Obata, S., Nishino, T., and Ogura, K. (1996) *Biochemistry* **35,** 9533–9538
14. Song, L., and Poulter, C. D. (1994) *Proc. Natl. Acad. Sci. U. S. A.* **91,** 3044–3048
15. Tarshis, L. C., Yan, M., Poulter, C. D., and Sacchettini, J. C. (1994) *Biochemistry* **33,** 10871–10877
16. Tarshis, L. C., Proteau, P. J., Kellogg, B. A., Sacchettini, J. C., and Poulter, C. D. (1996) *Proc. Natl. Acad. Sci. U. S. A.* **93,** 15018–15023
17. Ko, T. P., Chen, Y. K., Robinson, H., Tsai, P. C., Gao, Y.-G, Chen, A. P.-C., Wang, A. H.-J., and Liang, P. H. (2001) *J. Biol. Chem.* **276,** 47474–47482
18. Terwilliger, T. C., and Berendzen, J. (1999) *Acta Crystallogr. Sect. D Biol. Crystallogr.* **55,** 849–861
19. Guo, R. T., Ko, T. P., Chou, C. C., Shr, H. L., Chu, H. M., Tsai, Y. H., Liang, P. H., and Wang, A. H.-J. (2003) *Acta Crystallogr. Sect. D Biol. Crystallogr.* **59,** 2265–2268
20. Brunger, A. T., Adams, P. D., Clore, G. M., DeLano, W. L., Gros, P., GrosseKunstleve, R. W., Jiang, J.-S., Kuszewski, J., Nilges, M., Pannu, N. S., Read, R. J., Rice, L. M., Simonson, T., and Warren, G. L. (1998) *Acta Crystallogr. Sect. D Biol. Crystallogr.* **54,** 905–921
21. Fujii, H., Koyama, T., and Ogura, K. (1982) *Biochim. Biophys. Acta* **712,** 716–718
22. Ohnuma, S.-I., Narita, K., Nakazawa, T., Hemmi, H., Hallberg, A.-M., Koyama, T., Ogura, K., and Nishito, T. (1996) *J. Biol. Chem.* **271,** 10087–10095
23. Ohnuma, S.-I., Narita, K., Nakazawa, T., Ishida, C., Takeuchi, Y., Ohto, C., and Nishito, T. (1996) *J. Biol. Chem.* **271,** 30748–30754
24. Ohnuma, S.-I., Hirooka, K., Tsuruoka, N., Yano, M., Ohto, C., Nakane, H., and Nishito, T. (1998) *J. Biol. Chem.* **273,** 26705–26713
25. Chen, A., Kroon, P. A., and Poulter, C. D. (1994) *Protein Sci.* **3,** 600–607
26. Kainou, T., Okada, K., Suzuki, K., Nakagawa, T., Matsuda, H., and Kawamukai, M. (2001) *J. Biol. Chem.* **276,** 7076–7883
27. Guex, N., and Peitsch, M. C. (1997) *Electrophoresis* **18,** 2714–2723
28. Kraulis, P. J. (1991) *J. Appl. Crystallogr.* **24,** 946–950
29. Merritt, E. A., and Murphy, M. E. P. (1994) *Acta Crystallogr. Sect. D Biol. Crystallogr.* **50,** 869–873
30. Nicholls, A., Sharp, K. A., and Honig, B. (1991) *Proteins Struct. Funct. Genet.* **11,** 281–296